



TL 240 .A385 2000

ILL record updated to IN PROCESS
Record 6 of 11

ILL pe

Record 4 of 11

CAN YOU SUPPLY ? YES NO COND FUTUREDATE

:ILL: 7682471 :Borrower: IRQ :ReqDate: 20010417 :NeedBefore: 20010517
:Status: IN PROCESS 20010417 :RecDate: :RenewalReq:
:OCLC: 45670082 :Source: OCLCILL :DueDate: NIA :NewDueDate:
:Lender: *UMR,NED,TXH,IQU

:CALLNO:

:TITLE: Advanced vehicle technologies : presented at the 2000 ASME
International Mechanical Engineering Congress and Exposition, November 5-10,
2000, Orlando, Florida /

:IMPRINT: New York, N.Y. : American Society of Mechanical Engineers, c2000.

:SERIES: DE (Series) (American Society of Mechanical Engineers. Design
Engineering Division) ; vol. 106.

:ARTICLE: Mills, V;et al "Modeling, analysis, and experimental testing of ABS s
ystems..."

:VOL: 106 :NO: :DATE: :PAGES: 85-92

:VERIFIED: OCLC

:PATRON: Layton, Richard 191

:SHIP TO: ILL

Logan Library CM3
Rose-Hulman Institute of Technology
5500 Wabash Avenue
Terre Haute IN 47803-3999

:BILL TO: same/FEIN #35-086-8149

:SHIP VIA: ARIEL 137.112.60.14/INCOLSA WHEELS/bks lib rate/art fst cls

:MAXCOST: 5ifm :COPYRT COMPLIANCE: CCG

:BILLING NOTES: LVIS member

:BORROWING NOTES: Members please use INCOLSA WHEELS courier. Let me know
if maxcost is not enough and if there is a problem. THANK YOU.

:AFFILIATION: LVIS, CCC

:LOCATIONS: lcl

:LENDING CHARGES:

:SHIPPED:

:SHIP INSURANCE:

:LENDING RESTRICTIONS:

:LENDING NOTES:

:RETURN TO:

:RETURN VIA:

MODELING, ANALYSIS, AND EXPERIMENTAL TESTING OF ABS SYSTEMS WITH LOAD SHIFTING

Val Mills, Bernard Samuels, and Dr. John Wagner
Department of Mechanical Engineering
Clemson University, Clemson, SC

James Smith and Dr. Richard Layton
Department of Mechanical Engineering
North Carolina A&T State University, Greensboro, NC

Abstract

The steerability and stability of vehicles must be maintained during emergency stopping and evasive driving maneuvers on degraded roads. The introduction of antilock brake and traction control systems has expanded the envelope of safe vehicle operation. ABS development has traditionally depended on extensive in-vehicle testing, at proving grounds, which contribute to lengthy product development cycles. However, recent attention has focused on laboratory wheel testers and hardware-in-the-loop strategies to emulate test conditions in a controlled setting to shorten product design time and address critical safety issues. In this paper, the effect of transient load shifting due to cargo movement on ABS system performance will be studied. Analytical and empirical mathematical models are presented to describe the chassis, tire/road interface, wheel, and brake modulator dynamics. These models have been integrated into a simulation to allow the study of transient weight transfers on the vehicle's overall stopping distance and steerability. Experimental test results will be gathered on a single wheel tester which has been fabricated. The analysis of the numerical and experimental results will allow the ABS system performance to be predicted for various loading conditions and establish an envelope for safety critical testing during the product development process.

1. Introduction

The application of antilock brake and traction control systems (ABS/TCS) to passenger and commercial vehicles has expanded the envelope for maintaining control on degraded road surfaces. During emergency starting or stopping maneuvers on wet or ice covered roads, ABS/TCS systems can regulate the wheel spin through brake and/or engine intervention to maintain vehicle steerability and effect the requested acceleration or deceleration. ABS systems continually adjust the applied brake caliper pressure through the management of solenoid valves located in the brake modulator. For TCS functionality, a variety of strategies may be considered including fuel cutoff, spark retard, and/or brake intervention.

Furthermore, the availability of integrated ABS/TCS systems provide the opportunity to offer yaw control features to maintain vehicle stability during cornering maneuvers. In this instance, the driver's steering wheel commands are interpreted and compared against the vehicle's actual path with ensuing individual wheel braking and/or engine management to enhance realize the yaw envelope.

The modeling and analysis of ABS/TCS systems, prior to in-vehicle testing, requires the integration of automobile, environment, and driver dynamics to create a simulation tool. Vehicle chassis simulations (refer to Figure 1) typically include the platform, suspension, wheels, steering, brakes, tire/road interface, driver, environment, and in some instances, powertrain (i.e., engine and transmission) dynamics (Allen *et al.*, 1988). For instance, the wheel dynamic block is impacted by the transmission, brakes, and tire/road interface, and provides wheel speed (i.e., slip) information to the ABS controller and tire/road interface. For this project, analytical and empirical models have been developed to describe the dynamic behavior of light and medium-duty vehicles during emergency stopping maneuvers.

The primary components in a base brake system includes the master cylinder, vacuum assist boost, brake force valve, and brake calipers as shown in Figure 2 (Khan *et al.*, 1992). The driver's commanded brake pedal force is gained and transmitted to the brake calipers; the brake force valve proportions the brake pressure to the front and rear wheels to compensate for differing axle loadings. ABS systems supplement this base system with an electro-mechanical hydraulic modulator, four wheel speed sensors, and an electronic controller. The controller monitors each wheel speed signal for the onset of wheel lockup (i.e., wheel slip approaches unity) during braking maneuvers, and if present, regulates the brake pressure to that wheel. An important system variable that effects braking performance is variable axle loadings (i.e., tire normal force) due to vehicle pitch and cargo shifting.

To support the experimental testing of ABS systems, an automotive wheel, tire, and brake tester has been designed and

where A_D is the frontal area and C_D is the drag coefficient.

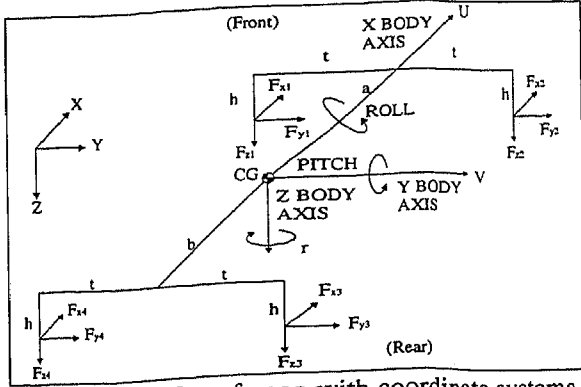


Figure 4. Platform forces with coordinate systems

The forces acting on the wheels, F_{xi} and F_{yi} , are functions of the wheel steer angle, δ_i , as well as the tire/road interface longitudinal F_{xwi} (i.e., wheel travel direction) and lateral F_{ywi} (i.e., normal to wheel travel direction) forces

$$F_{xi} = F_{xwi} \cos \delta_i - F_{ywi} \sin \delta_i \quad (8)$$

$$F_{yi} = F_{xwi} \sin \delta_i + F_{ywi} \cos \delta_i \quad (9)$$

The effective front wheel steer angle, δ_{FW} , becomes

$$\delta_{FW} = \frac{1}{2}(\delta_1 + \delta_2) \quad (10)$$

while the rear wheel steer angle, δ_{RS} , becomes

$$\delta_{RS} = -C_{SR} \phi \quad (11)$$

where C_{SR} is the roll-steer coefficient and ϕ is the sprung mass roll angle. In this paper, a quasi-static approximation has been selected for the latter

$$\phi = \frac{-hF_y}{K_{r\phi} + K_{f\phi}} \quad (12)$$

with h denoting the CG height, and $K_{r\phi}$ ($K_{f\phi}$) representing the front (rear) roll stiffness.

Tire/Road Interface: The vehicle traction force is dependent on the wheel slip, road surface, and normal load. The slip, λ , is defined as the ratio of the wheel's longitudinal and angular velocity to the longitudinal or angular velocity depending on whether the vehicle is accelerating or decelerating

$$\lambda_{decel} = \left(\frac{u_{wi} - R\omega_i}{u_{wi}} \right) \quad \text{and} \quad \lambda_{accel} = \left(\frac{u_{wi} - R\omega_i}{R\omega_i} \right) \quad (13)$$

As shown in Figure 5, the wheel slip is defined as $\lambda_{decel} = -1$ for full wheel spin with zero vehicle velocity and $\lambda_{accel} = 1$ for complete wheel lockup with finite vehicle velocity. Notice that maximum road surface traction, μ_{max} , generally occurs between 10-20% wheel slip (Gillespie, 1992).

The slip angle, α , is the angle between the vehicle's velocity vector and the tire's actual direction (Figure 6a)

$$\alpha_i = \tan^{-1} \left(\frac{v_i}{u_i} \right) - \delta_i \quad (14)$$

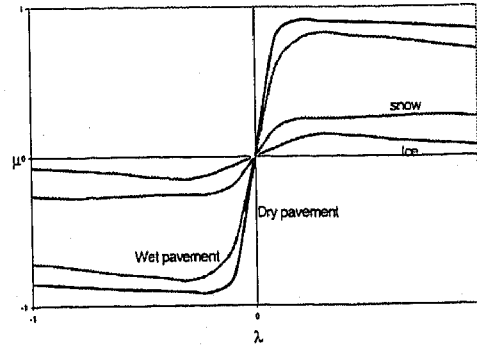


Figure 5. μ / λ curves for various road surfaces

A series of tire models will be presented to describe the longitudinal and lateral forces, as well as the aligning torques. The first model is an empirical representation based on the research by Bakker *et al.* (1987). The model inputs are the tire slip angle, normal wheel load, camber angle, road friction coefficient, wheel slip, and the steer angle. The model outputs are the lateral and longitudinal forces plus the aligning torque. The primary limitation of this model is that it applies only to pure cornering or braking under steady-state conditions.

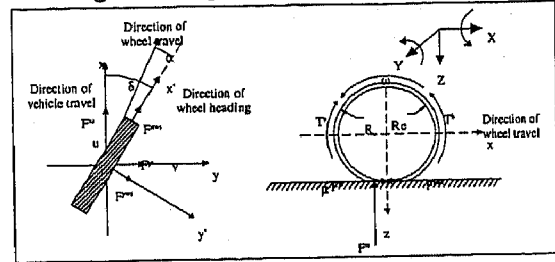


Figure 6. Schematic diagrams for (a) tires and (b) wheels

The longitudinal forces, lateral forces and aligning torques may be described by the general equation

$$Y = D \sin(C \arctan(B\phi)) \quad (15)$$

where the variable ϕ may be determined as

$$\phi = (1-E)X + (E/B) \arctan(BX) \quad (16)$$

When solving for the lateral force and aligning torque, the variable X represents the slip angle. However, when solving for the longitudinal force, the variable X represents the wheel slip. The coefficient C is practically independent of the vertical load F_x and is influenced mainly by the force/aligning torque of interest. The coefficients B , D , and E are dependent on both the vertical load and the quantity under consideration. These coefficients may be described, respectively, with the aid of a set of coefficients (i.e., a_i for $i=1,2,\dots,13$) that depend only on the force/aligning torque of interest. The values of B , D , and E for the longitudinal forces may be expressed as

$$B = \frac{a_3 F_z^2 + a_4 F_z}{C D e^{a_5 F_z}} \quad (17a)$$

$$D = a_1 F_z^2 + a_2 F_z \quad (17b)$$

$$E = a_6 F_z^2 + a_7 F_z + a_8 \quad (17c)$$

The lateral forces and aligning torques may be determined by a slight manipulation of equation (15) to add the effects of the camber angle γ . A vertical offset, S_v , must be added to compensate for the ply steer, conicity, and rolling resistance of the tire. Thus, equation (15) may be expressed as

$$Y = D \sin(C \arctan(B\phi)) + S_v \quad (18)$$

where S_v is dependent on the camber angle and normal load

$$S_v = \gamma (a_{10} F_z^2 + a_{11} F_z) \quad (19)$$

The variable ϕ may be determined using the slip angle as

$$\phi = (1 - E)\alpha + (E/B) \arctan(B\alpha) \quad (20)$$

The coefficient B is dependent on the camber angle

$$B = \frac{a_3 \sin(a_4 \arctan(a_5 F_z))}{C D} (1 - a_{12} |\gamma|) \quad (21)$$

The expressions for D and E for the lateral force are the same as equations (17b) and (17c), respectively.

The aligning torques M_z require the modification of the B and E coefficients as

$$B = \frac{a_3 F_z^2 + a_4 F_z}{C D e^{a_5 F_z}} (1 - a_{12} |\gamma|) \quad (22)$$

$$E = \frac{a_6 F_z^2 + a_7 F_z + a_8}{(1 - a_{12} |\gamma|)} \quad (23)$$

The various tire model coefficients are summarized in Table 1.

	F_x	F_y	M_z
a_1	-0.0213	-0.03430	-0.02710
a_2	1.1440	1.11500	-0.02820
a_3	4.9600	1.20720	-0.08870
a_4	22.6000	1.61530	0.07940
a_5	0.0690	0.20990	0.22530
a_6	-0.0060	0.03115	-0.07530
a_7	0.0560	-0.38400	0.75325
a_8	0.4860	0.81600	-1.70980
a_9	0	-1.00000	0.01500
a_{10}	0	-0.34440	-0.00066
a_{11}	0	1.72500	0.00945
a_{12}	0	0.08408	0.03000
a_{13}	0	0	0.07000
C	1.65	1.30	2.40

Table 1. Bakker tire model coefficients (F_z in kN)

Wheel Dynamics: The rotational dynamics for each wheel assembly depends on the applied engine drive torque, driver commanded brake torque, tire/road interface force, and viscous damping. To describe the motion, Newton's law may be written about the rotation axis

$$I_{wy} \dot{\omega}_i = T_i + F_{xwi}(R_e) - C_{wi} \omega_i \quad (24)$$

where I_{wy} is the moment of inertia of the wheel about the y-axis (refer to Figure 6b), ω is the wheel's angular velocity, T_i is the external applied torques, R_e is the effective tire radius, and C_w is the wheel damping coefficient.

The normal force, F_{zi} , accounts for the vehicle weight loading, as well as the dynamic affect of platform roll and pitch

$$F_{z1} = -\frac{mg}{2} \frac{b}{a+b} + \frac{hF_x}{2(a+b)} + \phi \frac{K_f \phi}{2t} \quad (25a)$$

$$F_{z2} = -\frac{mg}{2} \frac{b}{a+b} + \frac{hF_x}{2(a+b)} - \phi \frac{K_f \phi}{2t} \quad (25b)$$

$$F_{z3} = -\frac{mg}{2} \frac{a}{a+b} - \frac{hF_x}{2(a+b)} - \phi \frac{K_r \phi}{2t} \quad (25c)$$

$$F_{z4} = -\frac{mg}{2} \frac{a}{a+b} - \frac{hF_x}{2(a+b)} + \phi \frac{K_r \phi}{2t} \quad (25d)$$

Brake Subsystem: The base brake system contains the brake pedal with mechanical linkage to the master cylinder and vacuum assisted boost, proportional valve, and brake calipers (Gerdes *et al.*, 1993). Antilock brake systems typically contain five components: D.C. motor, hydraulic pump, fluid accumulator, and isolation and apply/release solenoids. The rear channel of an ABS system is shown in Figure 7 with master cylinder and wheel calipers. There are three standard system operating modes: standard brakes, pressure release, and pressure re-apply (Becker *et al.*, 1995).

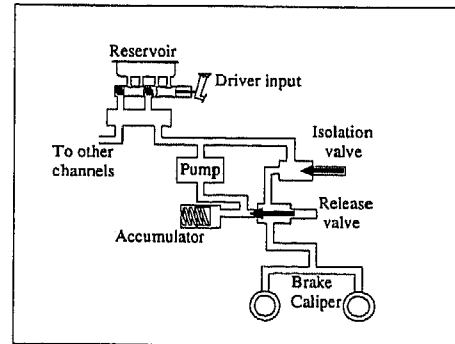


Figure 7. ABS system single channel configuration

The first mode allows brake pressure buildup to apply the brake calipers/drums. In this instance, the isolation solenoid is open and the apply/release pulse width modulated (PWM) solenoid is closed allowing fluid flow from the master cylinder to the brake calipers. The second operating mode corresponds to closure of the isolation solenoid and PWM solenoids. In this case, the isolation solenoid prevents the master cylinder from supplying fluid while the PWM solenoid prevents fluid travel from the brake caliper to the accumulator and/or pump. Finally, the third operating mode permits re-application of the brake pressure using an open isolation, operational pump, and pulsed PWM solenoid.

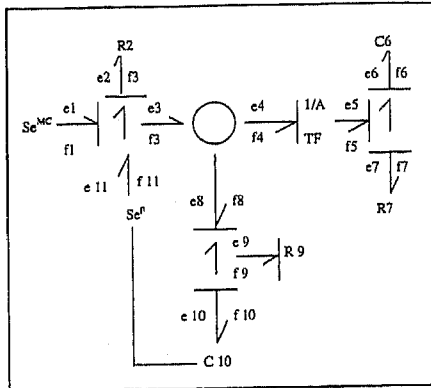


Figure 8. ABS system single channel bond graph

The ABS system displayed in Figure 7 was modeled using bond graphs per Figure 8 (Rosenberg and Karnopp, 1983). This analysis resulted in two differential equations for each channel (i.e., brake caliper piston displacement and fluid accumulator volume). In other words, a three channel (i.e., left front, right front, and rear) system requires six differential equations. The brake caliper piston displacement rate, \dot{q}_6 , may be expressed as

$$\dot{q}_6 = f_1 (f_2 q_{10} - f_3 q_6 + Se^{MC} + Se^P) \quad (26)$$

where q_{10} represents the fluid accumulator volume. The parameters Se^{MC} and Se^P denote the master cylinder and hydraulic pump pressures, respectively. The coefficient f_1 may be stated as

$$f_1 = AR_9 (A^2 R_2 R_9 + R_7 (R_2 + R_9))^{-1} \quad (27a)$$

where R_2 represents the isolation solenoid resistance, A is the brake caliper area, R_7 denotes the caliper resistance, and R_9 is the PWM solenoid resistance. The coefficient f_2 becomes

$$f_2 = (R_2 + R_9) (R_9 C_{10})^{-1} - C_{10}^{-1} \quad (27b)$$

where C_{10} represents the accumulator capacitance. Similarly, coefficient f_3 is calculated as

$$f_3 = \frac{(R_2 + R_9)}{AR_9 C_6} \quad (27c)$$

where C_6 denotes the brake caliper spring compliance.

The next differential equation describes the accumulator's volumetric flow rate, \dot{q}_{10}

$$\dot{q}_{10} = g_1 [g_2 (Se^{MC} + Se^P) - g_3 q_{10} - g_4 q_6] \quad (28)$$

Note that the volumetric flow rate is also a function of the brake caliper displacement, as well as the master cylinder and hydraulic pump pressures. In this instance, the coefficients g_1 through g_4 may be expressed as

$$g_1 = AR_2 (A^2 R_2 R_9 + R_7 (R_2 + R_9))^{-1} \quad (29a)$$

$$g_2 = \left(\frac{R_7}{AR_2} \right) \quad (29b)$$

$$g_3 = \left(\frac{R_7}{AR_2 C_{10}} \right) + \left(\frac{A}{C_{10}} \right) \quad (29c)$$

$$g_4 = \left(\frac{1}{C_6} \right) \quad (29d)$$

The ABS control system has been designed using a two-dimensional table (i.e., vehicle deceleration and wheel slip). Depending upon the value of these two input parameters, the brakes will operate in either normal mode, pressure isolation or pressure release. A model-based strategy will be implemented in the future to replace the model free approach.

Cargo Model: An important issue for light to medium-duty vehicles, carrying a payload as shown in Figure 9, is the accommodation of possible cargo shifting during emergency driving maneuvers. The base and ABS brake systems must be properly designed for load shifting which impacts the vehicle performance through the wheels' normal force, F_{zi} , per equation (25). Relative motion will occur between the payload and platform when the frictional force is insufficient to prevent movement. In other words, the payload mass may accelerate/decelerate differently than the platform mass causing horizontal/lateral displacement on the vehicle's bed. If this relative motion occurs during braking/launch, then the cargo's weight will be shifted toward the front/rear resulting in increased/decreased vehicle pitch, as well as potentially impacting the vehicle roll if yaw is also present. In addition to the weight shift, an impulsive force may arise due to the cargo impacting the front of the bed and ceasing relative motion. To properly accommodate this weight transfer, the ABS system must be designed to adapt to transient loading.

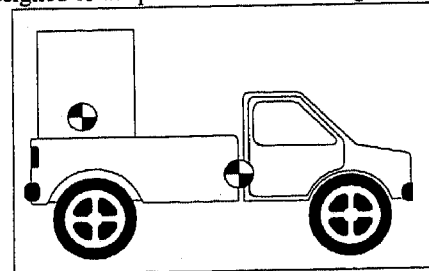


Figure 9. Cargo shifting for light-duty vehicle

A mathematical model has been derived to describe the dynamic motion of a payload resting on the vehicle's bed. The cargo model imposes two assumptions. First, although the payload motion may have longitudinal, lateral, vertical, and rotational components, it will be restricted to the longitudinal direction without rotation. In other words, the effect of lateral and yaw accelerations will not be considered. However, this constraint will be relaxed in subsequent research to enhance the weight transfer description. Second, the payload must continually remain in contact with the vehicle's bed and not "tip" over. The equations of motion for the vehicle's payload

- With the drivetrain clutch disengaged, motor is turned on.
- Clutch is engaged, bringing wheel and treadmill to speed.
- Clutch is disengaged, the motor is turned off, data acquisition is activated, and the braking system is actuated.

In operation, the drivetrain spins the tire and treadmill up to approximately 13 MPH. When the braking system is activated, the belt's inertia prevents it from coming to an immediate stop. This simulates a skid and allows the antilock feature of the ABS modulator to operate.

ABS Issues To Explore: Since the apparatus is an untested prototype, it is prudent to operate at low speeds. However, ABS operation requires speeds sufficiently high to permit an impending skid to occur. The treadmill design speed, 13 MPH, should satisfy these competing requirements. Treadmill deceleration in a skid is expected to be $24 \text{ (ft/s}^2\text{)}$ with a minimum stopping distance of 8 (ft). System instrumentation includes a pressure transducer at the master cylinder, a force and a displacement transducer at the brake pedal, an optical tachometer for the treadmill, and a wheel speed sensor. Future instrumentation may include a pressure transducer at the low pressure accumulator, a voltage (or current) sensor for the valve solenoids, a load cell on the treadmill support table, an angular accelerometer (or torque) transducer on the axle, and a linear treadmill accelerometer.

The apparatus can be used to study the effects on ABS performance of changes in the ABS controller, hydraulic lines, rotor or brake pads, and wheel orientation. In this paper, the term "performance" means all physical quantities of interest such as stopping distance, pressure transients, and noise. Specific components that can be evaluated in terms of these performance criteria are the electro-hydraulic control unit, brake pads and rotor, wheel orientation, hydraulic components, and the brake actuator. Pending hardware enhancements include the addition of a vertical force actuator to physically simulate the normal forces imposed on the wheel assembly.

4. Numerical Results

A comparison of the analytically estimated and experimental operational performance of an antilock brake system will be conducted when possible to validate the mathematical models and develop an ABS/TCS engineering design tool to study the effect of load shifting. A Matlab/Simulink™ simulation has been created to describe the dynamic behavior of a light-duty vehicle, equipped with ABS, during emergency braking maneuvers. For the purpose of this simulation, the vehicle parameters correlate to those of a 1988 Ford Ranger (Allen *et al.*, 1992).

An integration time-step of $\Delta t = 0.001$ seconds and Runge-Kutta integration routine were selected. In this paper, the primary focus will be the vehicle's longitudinal motion for different vehicle speeds, road surfaces, and base brakes with and without ABS intervention. Although a large number of

vehicle speeds, surfaces, loading, and brake combinations are possible, eight cases were initially selected (refer to Table 2).

	Vehicle Speed		Road Surface	Loading		Brakes	
	50 MPH	25 MPH		Normal	Shift	Base	ABS
1	X		Dry	X		X	
2	X		Dry	X		X	X
3	X		Dry		X	X	X
4	X		Wet	X		X	
5	X		Wet		X	X	X
6		X	Dry		X	X	
7		X	Wet	X		X	X
8		X	Dry/Wet		X	X	X

Table 2. Simulation test matrix

Figures 11-13 provide graphical responses of the left front and right rear wheel rotational velocities, vehicle longitudinal velocity, as well as the stopping distance for Cases 2, 3, and 5. An emergency stopping scenarios with ABS is shown in Figure 11. The road surface is dry with a nominal coefficient of friction of 1.05. Effects due to pitch causes the rear wheels to lock up before the front. The deceleration is 1.02 g's representing a 13% and 12% reduction in stopping distance and stopping time in comparison to Case 1. Notice that both wheel velocities show 5 departures as the ABS system regulates the deceleration through apply/release of the brake pressure.

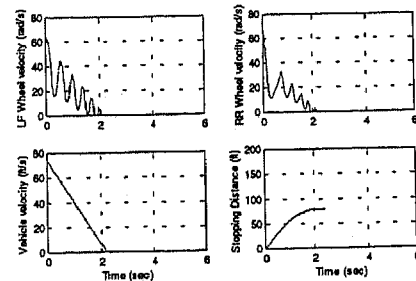


Figure 11. Dry pavement ABS stopping maneuver

Figure 12 demonstrates the result of cargo shifting during an emergency stopping maneuver with ABS on dry asphalt (Case 3). The weight shift causes an increase in stopping time of 18.2%, and an increase in stopping distance of 26.6% as compared with Case 2. At time $t=0.4$ seconds into the test, the cargo strikes the front of the cargo bed and ceases its relative motion. This results in an impact force modeled as an external impulse acting on the vehicle. This impulse is a contributing factor in the decrease of the vehicle deceleration to 0.92 g's .

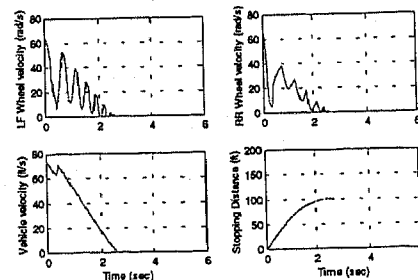


Figure 12. Dry pavement ABS stop with load shift

™ Registered trademarks of The MathWorks, Inc., Natick, MA

The change to a wet road surface with a friction coefficient of $\mu = 0.53$ results in a substantial decrease in the vehicle's stopping ability. In Figure 13 (Case 8), the ABS system must accommodate the transient effects of cargo shifting on the wet road surface at a lower speed. In comparison with Case 7 (i.e., wet asphalt ABS maneuver at low speed without load shift), the stopping time and stopping distance increase by 27.2% and 53.3%, respectively. Notice that the deceleration is 0.51 g's for Case 7 and 0.49 g's for Case 8, respectively.

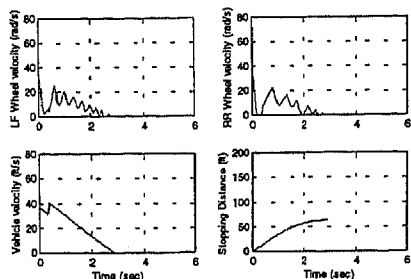


Figure 13. Wet pavement ABS stop with load shift

The vehicle deceleration results are summarized in Table 3.

5. Summary

The design of safety-critical automotive systems, such as antilock brake and traction control, are relying more heavily on simulation techniques to explore engineering issues before vehicle testing. In this paper, simulation and laboratory tools have been presented to investigate the effect of payload shifting on ABS system performance during emergency braking maneuvers. An eight degree-of-freedom chassis model, as well as a cargo model, were derived to describe the platform, tire/road interface, wheel dynamics, and payload. A six DOF model was described for the three channel D.C. motor solenoid-based ABS modulator. Eight representative simulation cases will be presented and discussed to highlight the tool's effectiveness.

A single wheel tester has been fabricated to support the laboratory testing and analysis of ABS systems under various operating conditions.

Case	Speed (mph)	Stopping Distance (ft)	Stopping Time (sec)	Wheel lockup
1	50	91.1	2.5	Yes
2	50	79.2	2.2	No
3	50	100.3	2.6	No
4	50	177.7	4.9	Yes
5	50	198.5	4.9	No
6	25	34.5	1.6	Yes
7	25	40.5	2.2	No
8	25	62.1	2.8	No

Table 3. Comparison of braking performance

References

- Allen, R. W., Rosenthal, T. J., and Szostak, H. T., "Analytical Modeling of Driver Response in Crash Avoidance Maneuvering, Volume I: Technical Background", U.S. Department of Transportation, Report DOT-HS-807-270, 1988.
- Allen, R.W., Szostak, H. T., Klyde, D. H., Rosenthal, T. J., and Owens, K. J., "Vehicle Dynamic Stability and Rollover", U.S. Department of Transportation, Report DOT-HS-807-956, 1992.
- Bakker, E., Nyborg, L., and Pacejka, H. B., "Tire Modeling for Use in Vehicle Dynamic Studies", SAE paper no. 870495, 1987.
- Becker, R., Sieger, E., Sowa, P., and Stegmaier, A., Automotive Brake Systems, Robert Bosch GmbH, 1995.
- Dugoff, H., Fancher, P.S., and Segel, L., "An Analysis of Tire Traction Properties and Their Influence on Vehicle Dynamic Performance", SAE paper no. 70377, 1970.
- Garrott, W. R., and Scott, R. A., "Improvement of Mathematical Models for Simulation of Vehicle Handling, Volume 7: Technical Manual for the General Simulation", U.S. Department Transportation, Report DOT-HS-805-370, 1980.
- Gerdes, J. C., Maciucă, D. B., Devlin, P. E., and Hedrick, J. K., "Brake System Modeling for IVHS Longitudinal Control", proceedings of the ASME Advances Robust Nonlinear Control Systems, New Orleans, LA, pp. 119-126, 1993.
- Gillespie, T. D., Fundamentals of Vehicle Dynamics, SAE, 1992.
- Hardy, M. S. A., and Cebon, D., "Investigation of Antilock Braking Strategies for Heavy Goods Vehicles", Proceedings of the Institution of Mechanical Engineers, Part D: Journal of Automobile Engineering, vol. 209, no. 4, pp. 263-271, 1995.
- Khan, Y., Kulkarni, P., and Youcef-Toumi, K., "Modeling, Experimentation, and Simulation of a Brake Apply System", proceedings of the American Controls Conference, Chicago, IL, pp. 226-230, 1992.
- Rosenberg, R. C., and Karnopp, D. C., Introduction to Physical System Dynamics, McGraw-Hill, NY, 1983.
- Tan, H. S., and Chin, Y. K., "Vehicle Traction Control: Variable Structure Control Approach", *ASME Journal of Dynamic Systems, Measurement, and Control*, vol. 113, no. 2, pp. 223-230, 1991.
- Wagner, J. and Keane, J., "A Strategy to Verify Chassis Controller Software - Dynamics, Hardware, and Automation", *IEEE Transactions on Systems, Man, and Cybernetics, Part A: Systems and Humans*, vol. 27, no. 4, pp. 480-493, 1997.